ELSEVIER

Neurobiology of Aging 33 (2012) 828.e19–828.e30

NEUROBIOLOGY OF AGING

www.elsevier.com/locate/neuaging

Functional connectivity tracks clinical deterioration in Alzheimer's disease

Jessica S. Damoiseaux[a,*], Katherine E. Prater[b], Bruce L. Miller[c], Michael D. Greicius[a]

[a] *Functional Imaging in Neuropsychiatric Disorders (FIND) Laboratory, Department of Neurology and Neurological Sciences, Stanford University School of Medicine, Palo Alto, CA, USA*

[b] *Neuroscience Graduate Program, University of Michigan, Ann Arbor, MI, USA*

[c] *Memory and Aging Center, Department of Neurology, University of California, San Francisco, CA, USA*

Received 21 December 2010; received in revised form 16 June 2011; accepted 23 June 2011

Abstract

While resting state functional connectivity has been shown to decrease in patients with mild and/or moderate Alzheimer's disease, it is not yet known how functional connectivity changes in patients as the disease progresses. Furthermore, it has been noted that the default mode network is not as homogenous as previously assumed and several fractionations of the network have been proposed. Here, we separately investigated the modulation of 3 default mode subnetworks, as identified with group independent component analysis, by comparing Alzheimer's disease patients to healthy controls and by assessing connectivity changes over time. Our results showed decreased connectivity at baseline in patients versus controls in the posterior default mode network, and increased connectivity in the anterior and ventral default mode networks. At follow-up, functional connectivity decreased across all default mode systems in patients. Our results suggest that earlier in the disease, regions of the posterior default mode network start to disengage whereas regions within the anterior and ventral networks enhance their connectivity. However, as the disease progresses, connectivity within all systems eventually deteriorates.

Keywords: Alzheimer's disease; Functional connectivity; Resting state fMRI; Disease progression; Default mode network; Fractionation

1. Introduction

Resting state functional connectivity changes within the default mode network, originally identified by Raichle et al. (Raichle et al., 2001), have been observed all across the spectrum from healthy aging (Andrews-Hanna et al., 2007; Damoiseaux et al., 2008), to mild cognitive impairment (Bai et al., 2009; Petrella et al., 2011; Sorg et al., 2007) to Alzheimer's disease (Gili et al., 2011; Greicius et al., 2004; Wang et al., 2007; Zhang et al., 2009). However, it is not yet known how functional connectivity changes in patients over time, as the disease progresses. A recent study investigated changes in functional connectivity across various stages of Alzheimer's disease (Zhang et al., 2010), using a cross-sectional design. However, a true longitudinal study of disease progression in Alzheimer's disease patients has not been performed to our knowledge.

Furthermore, while several studies have shown decreased functional connectivity within the default mode network in patients with mild to moderate Alzheimer's disease compared with healthy older controls (Greicius et al., 2004; Wang et al., 2007; Zhang et al., 2009) and patients with non-Alzheimer's disease dementia (Zhou et al., 2010), these studies have mainly focused on either 1 single default mode network (when using an independent component analysis (ICA) approach or on connectivity from a seed region in the posterior cingulate and/or precuneus cortex (in a cross-correlation approach). Recently it has been noted that the default mode network is not as homogenous as previ-

* Corresponding author at: Functional Imaging in Neuropsychiatric Disorders Lab, Department of Neurology and Neurological Sciences, Stanford University School of Medicine, 780 Welch Road, Suite 105, Palo Alto, CA 94304, USA. Tel.: +1 650 721 6136; fax: +1 650 724 4432.

E-mail address: jeske@stanford.edu (J.S. Damoiseaux).

0197-4580/$ – see front matter © 2012 Elsevier Inc. All rights reserved.
doi:10.1016/j.neurobiolaging.2011.06.024

Table 1
Demographics of Alzheimer's disease patients versus healthy elderly controls at baseline only

	AD patients	Controls	AD vs. controls (p)
Gender (m/f)	9/12	12/6	0.144
Education (y)[a]	16.1 ± 3.2	16.7 ± 3.0	0.583
Age (y)	64.2 ± 8.7	62.7 ± 10.3	0.631
MMSE	23.4 ± 4.2	29.2 ± 1.1	<0.001
Medications			
AD	Donepezil (n = 3) Memantine (n = 2) Donepezil and memantine (n = 6) Rivastigmine (n = 1)	—	
Antidepressants	SSRI (n = 4) SSRI and bupropion (n = 1) SNRI (n = 4) Trazodone (n = 1)	Bupropion (n = 1) SSRI (n = 1)	
Other	Zolpidem (n = 1) Alprazolam (n = 1)	—	

Key: AD, Alzheimer's disease; f, female; m, male; MMSE, Mini Mental State Examination; SSRI, selective serontonin reuptake inhibitor; SNRI, serotonin-norepinephrine reuptake inhibitor.
[a] Education information available in 18 patients and 13 controls.

ously assumed and several fractionations of the default mode network have been proposed (e.g., anterior vs. posterior or ventral vs. dorsal) (Andrews-Hanna et al., 2010; Leech et al., 2011; Qin et al., 2011; Uddin et al., 2009; Whitfield-Gabrieli et al., 2011). Here, we separately investigate the modulation of 3 default mode subnetworks, as identified with group ICA, by comparing Alzheimer's disease patients to healthy controls and by assessing connectivity changes over time.

Another limitation of most (but not all; Zhou et al., 2010) previous resting state functional magnetic resonance imaging (fMRI) studies on aging populations is that they have not controlled for gray matter atrophy. Gray matter atrophy is commonly observed in aging and dementia (Chan et al., 2001; Good et al., 2001) and can bias the results of functional activation or connectivity studies if not taken into account. Methodological limitations have most likely been the reason for omitting this gray matter correction in the past. Methods for analyzing resting state data are still evolving, as such existing methods are continuously being optimized and combined. It has now become easier to integrate information from multiple modalities, such as correcting fMRI maps on a voxel-by-voxel basis for differences in gray matter volume (Oakes et al., 2007). Here, we will demonstrate the importance of gray matter correction by showing our results with and without voxel-wise correction.

In short, in this study we aim to: (1) refine the previously observed changes in functional connectivity in patients with Alzheimer's disease by assessing these changes in 3 subnetworks of the default mode network; (2) demonstrate the effect of correcting voxel-wise for gray matter volume; and (3) examine functional connectivity changes in patients and healthy controls as the disease progresses.

2. Methods

2.1. Participants

This study consists of 2 partially overlapping datasets. The first dataset includes 21 Alzheimer's disease patients (data of 4 of the original 25 patients was excluded due to scanner artifacts) and 18 healthy elderly controls; see Table 1 for participant demographics and medication use. The second dataset is the longitudinal study. For this part of the study we asked the participants of the original (baseline) study to return for a second MRI session 2 to 4 years later. In total 11 patients and 10 controls returned. All follow-up scan data of 2 patients, and the anatomical scan data of 3 other patients and 2 healthy controls were excluded. Reasons for exclusion were poor data quality due to excessive motion and failure to collect data either due to time constraints or consideration of the patient's well-being (e.g., patients getting tired or anxious). As a result, the longitudinal study was divided into 2 datasets: 1 consisting of 9 patients and 10 controls used in the analyses without gray matter correction; and another consisting of 6 patients and 8 controls used in the analyses with gray matter correction. See Table 2 for the participant demographics of the longitudinal study.

Written, informed consent was obtained from patients directly, or from the legal guardian of any patients too impaired to provide informed consent. The Stanford University Institutional Review Board approved the study protocol. The patients were recruited from memory disorder clinics at Stanford University and the University of California San Francisco (UCSF). All patients met the National Institute of Neurological and Communicative Disorders and Stroke- Alzheimer's Disease and Related Disorders Association criteria for probable Alzheimer's disease (McKhann et al., 1984). The diagnosis of Alzheimer's disease at Stanford University and UCSF includes a diligent review of clinical brain imaging. Dementia patients with moderate to severe white matter

Table 2
Demographics of Alzheimer's disease patients and controls included in the longitudinal study

	AD patients		Controls		AD vs. controls (p)	
	Baseline	Follow-up	Baseline	Follow-up	Baseline	Follow-up
Gender (m/f)	4/2		7/1		0.386	
	[5/4]		*[9/1]*		*[0.098]*	
Education (years)[a]	17.6 ± 3.2		17.5 ± 2.9		0.958	
	[17.3 ± 3.5]		*[17.5 ± 3.1]*		*[0.882]*	
Age	66.5 ± 6.0	69.5 ± 5.9	63.1 ± 11.3	66 ± 10.8	0.520	0.489
	[67.7 ± 5.7]	*[70.6 ± 5.3]*	*[65.5 ± 11.1]*	*[69 ± 11.4]*	*[0.606]*	*[0.714]*
MMSE	26.0 ± 1.9	20.3 ± 7.1	29.5 ± 0.8	28.9 ± 1.6	0.000	0.006
	[25.2 ± 2.2]	*[17.4 ± 9.2]*	*[29.6 ± 0.7]*	*[28.8 ± 1.4]*	*[0.000]*	*[0.001]*
Time between baseline and follow-up (months)	35.5 ± 11.5		35.6 ± 12.9		0.985	
	[34.2 ± 12.2]		*[43.3 ± 19.8]*		*[0.252]*	

Data in italic is information of the groups as included in the analysis without gray matter correction.
Key: AD, Alzheimer's disease; f, female; m, male; MMSE, Mini Mental State Examination.
[a] Education information not available in 1 patient and 2 controls.

disease on T2 imaging are typically labeled as having a mixed dementia and are not included in research studies of Alzheimer's disease. Healthy controls were recruited from several sources (partners of patients, participants in a longitudinal study of normal aging at UCSF, and volunteers from the Stanford community). Exclusion criteria were having any significant medical, neurological (except for Alzheimer's disease in the patient group) or psychiatric illness, or a history of brain damage. All participants were right-handed. Baseline resting state fMRI data from most of these participants was used in a previous study examining whole-brain functional connectivity (Supekar et al., 2008); baseline data of 5 patients was used in Zhou et al., 2010; and baseline resting state data of all controls was used in Seeley et al., 2009.

2.2. Data acquisition

All imaging was performed at the Richard M. Lucas Center for Imaging at Stanford University on a 3-Tesla General Electric Signa (Milwaukee, WI) scanner using a standard whole-head coil. The scan session included both resting state fMRI and anatomical MRI. For the resting state functional scan, 180 volumes of 28 axial slices (4 mm thick, 1 mm skip) were acquired parallel to the plane connecting the anterior and posterior commissures and covering the whole brain using a T2* weighted gradient echo spiral in/out pulse sequence (repetition time = 2000 ms, echo time = 30 ms, flip angle = 80 degrees and 1 interleave) (Glover and Law, 2001). For the resting state scan, subjects were instructed to lie still with their eyes closed, not to think of any 1 thing in particular and not to fall asleep. In all subjects 2 of these 6-minute resting state runs were collected. For the anatomical scan a high resolution T1-weighted spoiled gradient recalled 3-D MRI sequence with the following parameters was used: 124 coronal slices 1.5-mm thickness, no skip, repetition time = 11 ms, echo time = 2 ms, and flip angle = 15 degrees.

2.3. Data analysis

2.3.1. Preprocessing of resting state data

Image preprocessing was carried out using tools from FMRIB's Software Library (FSL; version 4.1) (Smith et al., 2004). The following prestatistics processing was applied: motion correction (Jenkinson et al., 2002); removal of nonbrain structures (Smith, 2002); spatial smoothing using a Gaussian kernel of 6-mm full width at half maximum; mean-based intensity normalization of all volumes by the same factor (i.e., 4-dimensional grand-mean scaling in order to ensure comparability between data sets at the group level); high-pass temporal filtering (Gaussian-weighted least squares straight line fitting, with σ = 75.0 seconds); and Gaussian low-pass temporal filtering (half width at half maximum 2.8 seconds). After preprocessing, the functional scan was first aligned to the individual's high resolution T1-weighted image, which was subsequently registered to the MNI152 standard space (average T1 brain image constructed from 152 normal subjects at Montreal Neurological Institute) using affine linear registration (Jenkinson et al., 2002). The intermediate step in the alignment process was not performed for the 5 subjects whose anatomical scan was excluded from the analyses.

2.3.2. Preprocessing of anatomical data

After removal of nonbrain structures (Smith, 2002) the high-resolution images (T1-weighted spoiled gradient recalled) were segmented into gray matter, white matter, cerebrospinal fluid, and background, and partial volume maps were calculated (Zhang et al., 2001). All individual subjects' gray matter partial volume maps were transformed into MNI152 standard space using affine linear registration and a 4-dimensional image was created by concatenating every individual's standard space gray matter image.

2.3.3. Statistical analysis

The dual regression technique as described in (Filippini et al., 2009; Veer et al., 2010) was used to perform voxel-wise between group comparisons of resting state connectivity. This approach entails 3 steps: first, creating data-driven population-specific spatial maps showing large-scale connectivity patterns, by running group ICA on the concatenated resting state data of both the Alzheimer's disease patients and healthy controls combined. In this analysis, the dataset was decomposed into 25 independent components. Second, performing the actual dual regression by (1) using all the 25 independent components in a linear model fit (spatial regression) against the individual data, resulting in specific time courses for each independent component and subject, and (2) using these time courses in a linear model fit (temporal regression) against the individual's resting state data to estimate subject-specific spatial maps. Lastly, performing voxel-wise between group statistical testing on the subject-specific spatial maps using nonparametric permutation testing (5000 permutations) (Nichols and Holmes, 2002). To control for differences in gray matter volume, the individual gray matter partial volume maps at baseline and follow-up (if applicable) were included as a voxel-wise regressor in the between-group comparison, as described by (Oakes et al., 2007) and implemented in FSL. The first step (group ICA) was performed using the first run of the baseline resting state data of all patients and controls combined. The resulting 25 independent components were used in the next dual regression steps for all 6 subanalyses (i.e., baseline patient vs. baseline control; baseline patient vs. follow-up patient; and baseline control vs. follow-up control; for each resting state run separately), to keep the spatial patterns consistent across subanalyses. After running the actual dual regression steps but before running the between-group statistics, the individual functional connectivity maps of the 2 resting state runs were averaged creating a mean connectivity map per subject per time point. See Supplementary Fig. 1 for a graphical representation of the data analysis approach.

The default mode network and a control network in which we did not expect to find any changes at baseline (i.e., the sensorimotor network) were selected for between-group analyses. In line with previous observations (Damoiseaux et al., 2008), 3 out of the 25 group independent components could visually and methodologically be identified as the default mode network (i.e., the top 3 best-fits using the template matching procedure described by Greicius et al. on the group ICA results, using the default mode network reported in Damoiseaux et al. as template; Damoiseaux et al., 2006; Greicius et al., 2004). In order to assess any potential differences in modulation of these networks, we included all 3 default mode subnetworks in the analysis. The first best-fit is referred to by us as the "posterior default mode network" as it encompasses a prominent posterior cingulate/precuneus cluster, clusters in the lateral parietal and middle temporal gyrus, and additional smaller clusters in the anterior cingulate, superior, and middle frontal gyri. The second best-fit, which we refer to as the "ventral default mode network", encompasses a large ventrally located cluster extending from the precuneus and posterior cingulate, via the retrosplenial cortex into the parahippocampal gyrus and thalamus, with additional clusters in the medial frontal cortex, superior and middle frontal gyri, and posterior insula. Lastly the third best-fit, the "anterior default mode network", includes a sizeable frontal cluster, and additional clusters in the anterior and posterior cingulate, precuneus, occipitoparietal, temporal pole, and hippocampus. For the sensorimotor network 1 independent component was identified. See Fig. 1 for a visual representation of the networks of interest and Supplementary Table 1 for further details.

To find significant differences between Alzheimer's patients and controls at baseline, a 2-sample t test was performed, using "threshold-free cluster enhancement" (TFCE) as implemented in FSL (Smith and Nichols, 2009) with $p < 0.05$ family-wise error corrected, and spatially masked with the thresholded group ICA component in question (posterior probability threshold of $p > 0.5$). For the longitudinal study, a repeated measures analysis was performed testing for the difference between baseline and follow-up per group and for the group $\times$ time interaction, using TFCE; $p < 0.01$ uncorrected; and spatially masked with the thresholded group ICA component in question.

3. Results

3.1. Alzheimer's disease patients versus healthy controls at baseline

At our baseline measurement functional connectivity in Alzheimer's disease patients compared with controls was differentially modulated across the 3 default mode networks. In line with previous research, we found significantly decreased connectivity in patients in the posterior default mode network, more specifically in the left precuneus cortex. However, patients showed significantly increased connectivity in both the ventral (i.e., in the precuneus) and anterior (i.e., in the frontal pole) default mode networks (Table 3, Fig. 2). No significant between-group differences were observed in the opposite contrasts, or in the sensorimotor network. Correcting for gray matter volume by adding it as a voxel-wise covariate to the between-group analysis did influence the results. The specific brain areas showing differences remained the same but the cluster size changed. For the anterior and posterior default mode network the cluster size of significant voxels was smaller with correction, for the ventral default mode network the cluster size was bigger with correction (see Fig. 2 and Supplementary Table 2).

3.2. Longitudinal study

Patients with Alzheimer's disease showed significantly decreased connectivity in all 4 resting state networks at

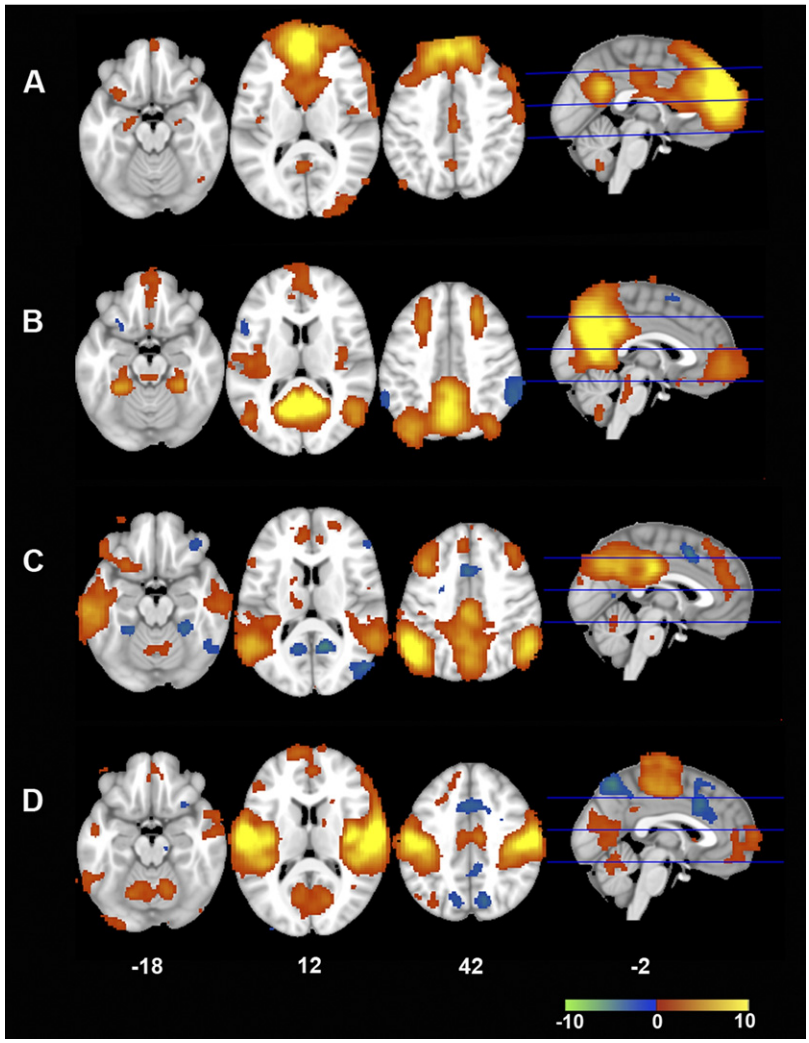

Fig. 1. Group independent component analysis (ICA) z-stat maps of the 3 default mode networks and the sensorimotor network. The group independent components selected for between-group statistics include 3 networks of interest: (A) anterior; (B) ventral; and (C) posterior default mode network; and (D) the sensorimotor network as a control. Shown here using a posterior probability threshold of $p > 0.5$; Montreal Neurological Institute (MNI) coordinates axial slices: $z = -18, 12, 42$.

follow-up compared with baseline in both analyses with and without gray matter correction (Fig. 3, left panel). In the anterior default mode network these decreases were mainly found in the superior frontal gyrus; in the ventral default mode network decreases were found in the lingual gyrus and/or precuneus cortex; in the posterior default mode de-

Table 3
Brain clusters showing differences between Alzheimer's disease patients and controls at baseline after correcting for gray matter density

Brain network	Contrast	Brain region	Cluster size (voxels)[a]	Peak MNI coordinates (mm)		
				X	Y	Z
Anterior DMN	AD > control	LH frontal pole	3185	−10	58	4
		RH frontal pole	42	24	36	44
		LH sup frontal gyrus	26	−8	22	56
Ventral DMN	AD > control	LH precuneus cortex	578	−6	−56	54
		RH precuneus cortex	49	4	−58	40
Posterior DMN	Control > AD	LH precuneus cortex	151	−4	−68	34

Key: AD, Alzheimer's disease; DMN, default mode network; LH, left hemisphere; MNI, Montreal Neurological Institute; RH, right hemisphere; sup, superior.

[a] Only clusters > 20 voxels are displayed here.

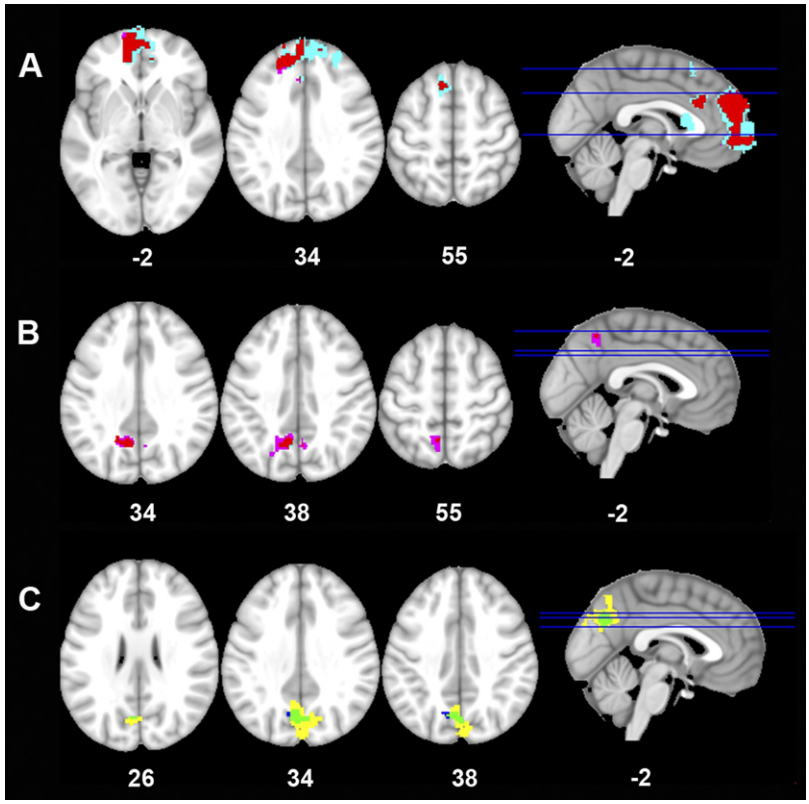

Fig. 2. Functional connectivity difference maps of Alzheimer's patients versus healthy elderly controls at baseline. Functional connectivity differences between Alzheimer's patients and healthy elderly controls in the (A) anterior; (B) ventral; and (C) posterior default mode network. The different colors represent the results with and without gray matter correction and the overlap between the 2. Functional connectivity in the anterior and ventral default mode networks (A) and (B) is increased in Alzheimer's patients compared with controls (displayed in violet for results with gray matter correction; in cyan for results without correction; and in red for the overlap). Functional connectivity in the posterior default mode network (C) is decreased (displayed in blue for results with gray matter correction (only visible for a few voxels here); in yellow for results without correction; and in green for the overlap). The statistical maps, thresholded using TFCE and $p < 0.05$ family-wise error corrected, are overlaid on the MNI152 brain; Montreal Neurological Institute (MNI) coordinates (in mm) of the slices are displayed.

creases were found in the middle temporal gyrus; and in the sensorimotor network decreases were found in the pre- and postcentral gyri. Increased connectivity in patients was also observed in small clusters in the posterior default mode and sensorimotor network.

Healthy controls also showed decreased functional connectivity at follow-up compared with baseline in the 3 default mode networks both with and without gray matter correction. No decreased functional connectivity was observed in the sensorimotor network with gray matter correction; a small cluster was found in the left frontal pole without gray matter correction (see Fig. 3, right panel).

In Fig. 4 we show the connectivity changes observed in Alzheimer's patients that are significantly different from the changes observed in healthy controls. As illustrated by the bar graphs in Fig. 4 (of the results with gray matter correction), the decrease in functional connectivity in these regions over time is greater in Alzheimer's patients than in controls. Most of these clusters actually show an increase in connectivity over time in healthy controls, except for 1 region in the posterior default mode and 2 regions in the sensorimotor network. All longitudinal results with gray matter correction are presented in Table 4, and all longitudinal results without gray matter correction are presented in Supplementary Table 3.

4. Discussion

The decrease in functional connectivity observed in the precuneus region of the posterior default mode network in patients with Alzheimer's disease compared with healthy elderly controls is what we expected to find considering the existing literature (Greicius et al., 2004; Sorg et al., 2009; Wang et al., 2006; Zhou et al., 2010). The finding of increased connectivity in the anterior and ventral default mode networks has not been reported as such. Both increased and decreased default mode connectivity has previously been observed in patients with mild cognitive impairment versus healthy controls (Qi et al., 2010), but no reference to a specific default mode subnetwork was made. The observed increased functional connectivity in the anterior default mode network is concordant with a previous

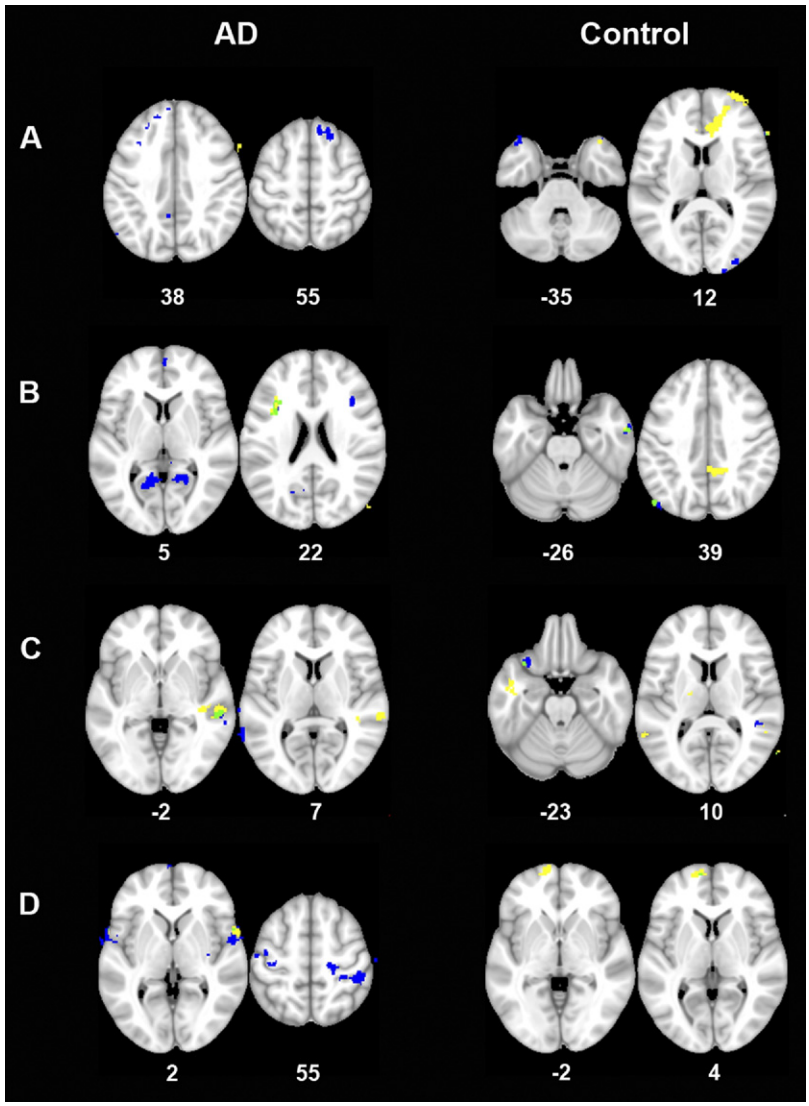

Fig. 3. Functional connectivity reductions in Alzheimer's disease patients and healthy controls at follow-up compared with baseline. Functional connectivity decreases in both Alzheimer's patients (left panel) and healthy elderly controls (right panel) at follow-up compared with baseline in the (A) anterior, (B) ventral, and (C) posterior default mode network, and (D) the sensorimotor network. The different colors represent the results with and without gray matter correction and the overlap between the 2. Displayed in blue are the results with gray matter correction; in yellow the results without correction; and in green the overlap. The statistical maps, thresholded using threshold-free cluster enhancement (TFCE) and $p < 0.01$ uncorrected, are overlaid on the MNI152 brain; Montreal Neurological Institute (MNI) coordinates (in mm) of the slices are displayed.

study from our group that applied a distinct analysis of whole-brain connectivity across 90 brain regions to a largely overlapping set of subjects (Supekar et al., 2008). That study showed disrupted local connectivity in Alzheimer's patients, with mainly decreased correlations within the temporal lobe and between the temporal lobe and other cortical and subcortical regions, and, importantly, increased connectivity within the frontal lobe. Our current findings confirm these previous results and show that they hold when using both a completely distinct analysis, which includes 3 default mode subnetworks, and when correcting for gray matter volume. The increased connectivity in the precuneus region of the ventral default mode network is more difficult to understand and corroborate. The histological studies by Braak and Braak show that the pathology in Alzheimer's disease takes place in several stages, affecting the medial temporal lobe first followed by posterolateral cortical regions and moving in the latest stages into the frontal cortex (Braak and Braak, 1991). In line with this research we would expect the ventral default mode network to be one of the first networks to develop neurofibrillary tangles, because of its involvement of the medial temporal lobe. Our results suggest that earlier in the disease, areas within the posterior default mode system start to disengage whereas areas within the ventral and anterior systems seem more connected. As the disease progresses, connectivity within the latter (and

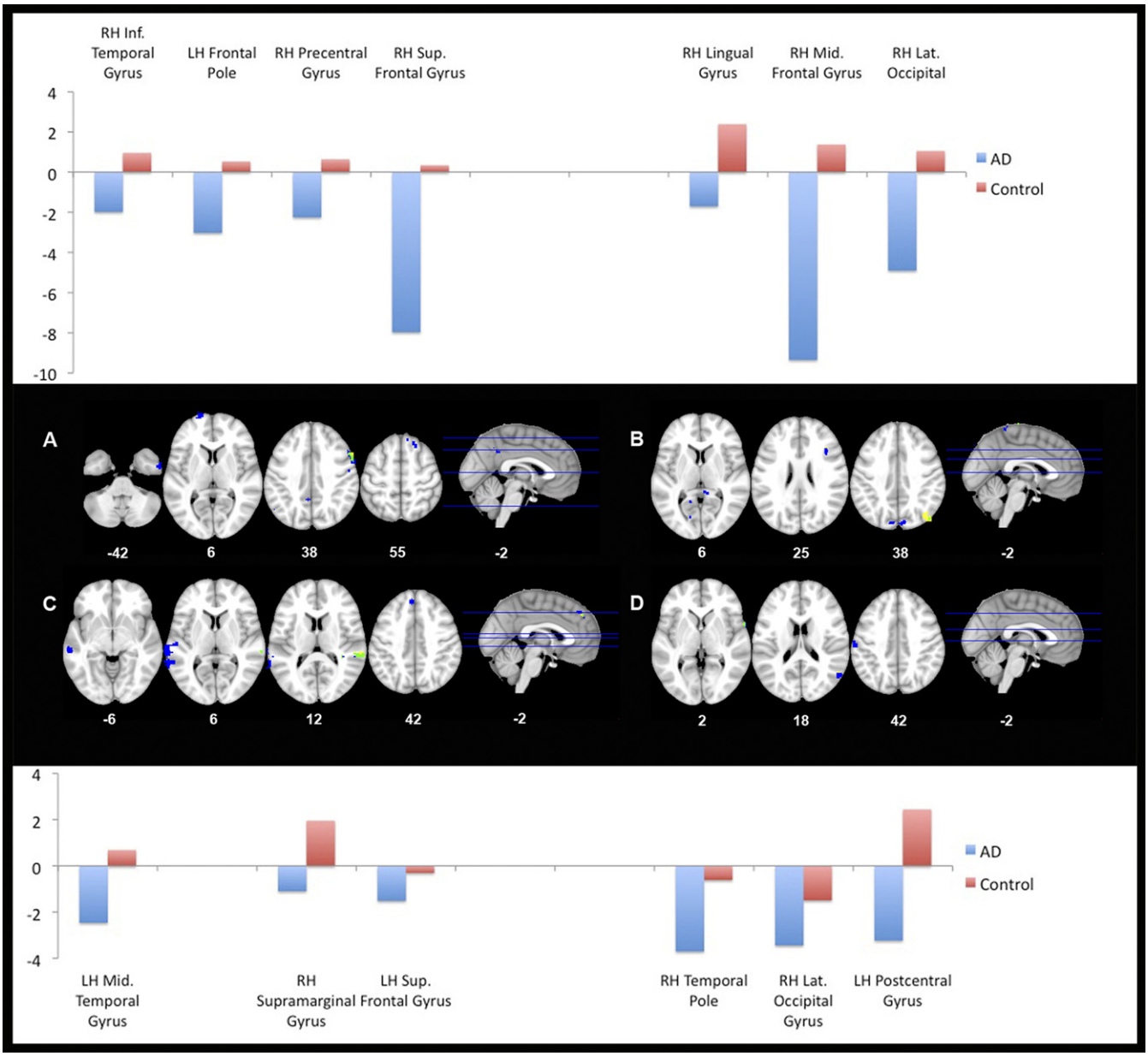

Fig. 4. Differential functional connectivity changes between Alzheimer's disease patients and healthy elderly controls over time. Regions in which the functional connectivity changes over time are significantly different in Alzheimer's patients than in healthy elderly controls, for the (A) anterior, (B) ventral, and (C) posterior default mode network, and (D) the sensorimotor network. The different colors represent the results with and without gray matter correction and the overlap between the 2. Displayed in blue are the results with gray matter correction; in yellow the results without correction; and in green the overlap. The statistical maps, thresholded using threshold-free cluster enhancement (TFCE) and $p < 0.01$ uncorrected, are overlaid on the MNI152 brain; Montreal Neurological Institute (MNI) coordinates (in mm) of the slices are displayed. To show the directionality of the effects, bar graphs are included. The anterior and ventral default mode networks are displayed above the corresponding brain images; for the posterior default mode and sensorimotor network they are displayed below the corresponding brain images. Bar graphs display the mean raw t statistic of selected regions in the specific network for the follow-up > baseline contrast in patients and controls separately.

other) systems eventually deteriorates, as shown in our longitudinal study.

In our longitudinal study we specifically tested whether the observed connectivity changes in Alzheimer's patients were different from those observed in healthy controls. Across all 3 default mode networks and the sensorimotor network we found significantly different changes over time, i.e., we found more decreased connectivity at follow-up in patients with Alzheimer's disease than in controls. Interestingly, most brain clusters that showed a decrease in patients over time showed an increase in controls. Although very tentative, this could support the theory that functional compensation already starts in healthy aging. Increases in task-induced activity

Table 4
Brain clusters showing longitudinal differences in Alzheimer's disease patients and controls after gray matter density correction

Group	Brain network	Contrast	Brain region	Cluster size (voxels)[a]	Peak MNI coordinates (mm)		
					X	Y	Z
AD patients	Anterior DMN	Baseline > follow-up	RH superior frontal gyrus	90	20	24	56
	Ventral DMN	Baseline > follow-up	LH lingual gyrus	225	−6	−56	0
			RH precuneus cortex	157	18	−56	6
			RH middle frontal gyrus	53	40	20	24
			LH inferior frontal gyrus	51	−36	16	20
			RH cuneal cortex	50	10	−84	40
			RH paracingulate gyrus	32	10	54	−4
		Follow-up > baseline	LH cerebral white matter	29	−26	8	38
	Posterior DMN	Baseline > follow-up	LH middle temporal gyrus	76	−66	−50	2
			RH middle temporal gyrus	38	56	−32	−2
	Sensorimotor	Baseline > follow-up	RH precentral gyrus	543	68	4	4
			RH supramarginal gyrus	338	54	−28	46
			LH postcentral gyrus	191	−46	−30	46
			LH superior temporal gyrus	101	−66	2	−8
			RH middle temporal gyrus	84	64	−10	−10
			RH postcentral gyrus	76	58	−4	30
			LH inferior frontal gyrus	32	−56	12	6
			LH precentral gyrus	28	−36	−24	56
			RH paracingulate gyrus	21	10	50	10
			RH postcentral gyrus	21	16	−32	78
			LH postcentral gyrus	21	−38	−20	42
		Follow-up > baseline	RH juxtapositional lobule cortex	51	2	−8	70
Controls	Anterior DMN	Baseline > follow-up	LH temporal pole	63	−38	20	−36
			RH occipital pole	33	32	−92	12
			RH occipital pole	28	20	−102	10
	Ventral DMN	Baseline > follow-up	LH lateral occipital cortex	48	−52	−76	38
			RH middle temporal gyrus	34	64	−2	−28
	Posterior DMN	Baseline > follow-up	LH frontal orbital cortex	81	−32	22	−20
Interaction group × time	Anterior DMN	Change in AD ≠ change in controls	RH precentral gyrus	186	60	−6	46
			LH frontal pole	61	−20	74	6
			RH inferior temporal gyrus	31	54	−2	−42
			RH lateral occipital cortex	31	46	−80	−6
			LH lateral occipital cortex	23	−52	−72	20
			RH superior frontal gyrus	22	20	26	56
	Ventral DMN	Change in AD ≠ change in controls	RH lingual gyrus	64	8	−40	−4
			RH lateral occipital cortex	32	10	−84	42
			LH postcentral gyrus	21	−2	−42	68
	Posterior DMN	Change in AD ≠ change in controls	LH middle temporal gyrus	419	−60	−28	−6
			LH superior frontal gyrus	44	−4	44	42
			RH supramarginal gyrus	32	60	−38	12
			RH planum temporale	30	36	−36	18
			LH middle temporal gyrus	26	−62	−12	−12
	Sensorimotor	Change in AD ≠ change in controls	LH postcentral gyrus	56	−58	−22	44
			RH lateral occipital cortex	41	58	−62	18
			LH middle temporal gyrus	34	−66	2	−10
			RH temporal pole	33	62	8	2

Key: AD, Alzheimer's disease; DMN, default mode network; LH, left hemisphere; MNI, Montreal Neurological Institute; RH, right hemisphere.
[a] Only clusters > 20 voxels are displayed here.

have frequently been observed in healthy aging and have been attributed to functional compensation (Cabeza et al., 2002; Davis et al., 2008; Dennis and Cabeza, 2008). The observed increases in functional connectivity in this study could potentially reflect the same phenomenon.

As expected, the sensorimotor network did not show any changes at baseline. However, our results suggest that when patients reach moderate to severe Alzheimer's disease, even connectivity between sensorimotor regions is affected.

The involvement of the precuneus and/or posterior cingulate cortex in multiple independent components, plus the observation of differential changes in adjacent areas of the precuneus and/or posterior cingulate cortex in a patient population across these independent components provides further support for the previously proposed functional fractionation of this brain area (Leech et al., 2011). The decomposition of the default mode network into multiple networks as seen in the current study has been observed previously

(Damoiseaux et al., 2008; Littow et al., 2010; Westlye et al., 2011). ICA may not always split the default mode network into several components, it can depend, among other factors, on the number of components the analysis outputs, the number of subjects, and the specific set of subjects (Abou-Elseoud et al., 2010). Nevertheless, the subdivision of the default mode network has also been observed when applying different analysis approaches, such as region-of-interest based cross-correlations (Andrews-Hanna et al., 2010; Uddin et al., 2009). Recently, subdivisions of the default mode system have been associated with distinct cognitive functions. The specific cognitive attributions vary somewhat across studies but broadly speaking they support the notion that the anterior default mode network is mainly involved in self-referential processing; the posterior default mode in familiarity and/or autobiographical memory; and the ventral network in constructing a mental scene based on memory (Andrews-Hanna et al., 2010; Qin et al., 2011; Uddin et al., 2009; Whitfield-Gabrieli et al., 2011). We would expect that the networks more directly involved with memory function are the first ones to deteriorate in patients with Alzheimer's disease. The posterior network does show signs of deterioration, but the ventral default mode network does not, connectivity even increases. Future research is needed to clarify the observed changes in this network. Overall, we believe the current results, along with results from previous studies, imply that the subdivision of the default mode network is functionally relevant and not merely a methodological artifact.

In this manuscript we have presented the results of our between-group analyses both with and without applying a voxel-wise gray matter correction. The effect of this correction appears substantial but not straightforward. Overall the same brain areas show significant changes both with and without correction and only the size of these areas differs. However, the effect of the correction on cluster size is observed to go in either direction (i.e., either larger or smaller after correction). The observation of a smaller area showing functional connectivity changes after gray matter correction seems most intuitive, i.e., the observed decreases in functional connectivity actually reflect decreases in gray matter volume. Nonetheless, our data suggest that gray matter volume differences can also hide functional changes. Regardless of the directionality of the effect of gray matter correction, this study illustrates its importance and we believe a gray matter correction should be included in all fMRI studies involving aging populations.

A limitation of the current study is the small number of subjects included in the longitudinal study. Although we attempted to mitigate this limitation by collecting two 6-minute resting state runs per subject and averaging the resulting connectivity maps per subject, the longitudinal results should be considered preliminary until validated in a larger number of subjects. An additional limitation pertains to the rather long interval (3 years on average) between scans. Ongoing studies in our laboratory, and probably in other laboratories as well, will determine whether significant changes in connectivity can be detected over shorter intervals of 1 year or less. We expect that differences in connectivity will be detectable at shorter intervals given that those detected here reflect reduced connectivity even after accounting for loss of gray matter volume. A third limitation could be that our specific group of Alzheimer's patients show a larger than average increase in functional connectivity because of their relatively high education level. It is observed clinically that people with a high premorbid IQ do better with a given degree of focal cognitive dysfunction (Bruandet et al., 2008). In addition, several studies have shown structural and/or functional imaging correlates of such cognitive reserve (Serra et al., 2011; Solé-Padullés et al., 2009). It would be interesting for future research to examine the effect of cognitive reserve on functional connectivity by, e.g., testing if Alzheimer's patients with a high education level show more increased connectivity than patients with a low education level.

The current results suggest that resting state functional connectivity in the default mode system changes differentially across its subnetworks as Alzheimer's disease progresses. In addition, our results support the possibility that compensatory increases in connectivity occur in regions, like the frontal cortex, that are relatively preserved early in the disease. As the disease progresses, however, these regions become targeted by Alzheimer's disease pathology and their connectivity also declines. These interpretations are based on studies comparing Alzheimer's disease patients with healthy older controls. It would be interesting to examine the trajectory of default mode connectivity changes in healthy people at risk for Alzheimer's disease. One known risk factor for Alzheimer's disease is the presence of the apolipoprotein E4 allele (*APOE*-ε4) (Strittmatter et al., 1993). Two recent studies showed functional connectivity changes in areas of the default mode network in healthy young *APOE*-ε4 carriers (Filippini et al., 2009) and healthy older *APOE*-ε4 carriers (Sheline et al., 2010) compared with noncarriers. It would be interesting to investigate whether the differential modulation of the default mode's subnetworks, as demonstrated here in Alzheimer's patients, can also be observed in *APOE*-ε4-carriers.

To our knowledge, this is the first longitudinal study showing a differential modulation of 3 default mode subnetworks in patients with Alzheimer's disease. With continued advances in methodology, we expect that resting state fMRI may prove useful as a marker of Alzheimer's disease progression and ideally, when disease-modifying treatments become available, disease regression.

Disclosure statement

The authors disclose no conflicts of interest.

Written, informed consent was obtained from patients

directly or from the legal guardian of any patients too impaired to provide informed consent. The Stanford University Institutional Review Board approved the study protocol.

Acknowledgements

This work was supported by a grant from the John Douglas French Foundation and the following NIH grants: RO1NS073498, P01AG019724, and P50AG023501. The authors thank Gary Glover for his acquisition expertise and attention to scanner stability over time.

Appendix A. Supplementary data

Supplementary data associated with this article can be found, in the online version, at doi:10.1016/j.neurobiolaging.2011.06.024.

References

Abou-Elseoud, A., Starck, T., Remes, J., Nikkinen, J., Tervonen, O., Kiviniemi, V., 2010. The effect of model order selection in group PICA. Hum. Brain Mapp. 31, 1207–1216.

Andrews-Hanna, J.R., Reidler, J.S., Sepulcre, J., Poulin, R., Buckner, R.L., 2010. Functional-anatomic fractionation of the brain's default network. Neuron 65, 550–562.

Andrews-Hanna, J.R., Snyder, A.Z., Vincent, J.L., Lustig, C., Head, D., Raichle, M.E., Buckner, R.L., 2007. Disruption of large-scale brain systems in advanced aging. Neuron 56, 924–935.

Bai, F., Watson, D.R., Yu, H., Shi, Y., Yuan, Y., Zhang, Z., 2009. Abnormal resting-state functional connectivity of posterior cingulate cortex in amnestic type mild cognitive impairment. Brain Res. 1302, 167–174.

Braak, H., Braak, E., 1991. Neuropathological stageing of Alzheimer-related changes. Acta Neuropathol. 82, 239–259.

Bruandet, A., Richard, F., Bombois, S., Maurage, C.A., Masse, I., Amouyel, P., Pasquier, F., 2008. Cognitive decline and survival in Alzheimer's disease according to education level. Dement. Geriatr. Cogn. Disord. 25, 74–80.

Cabeza, R., Anderson, N.D., Locantore, J.K., McIntosh, A.R., 2002. Aging gracefully: compensatory brain activity in high-performing older adults. Neuroimage 17, 1394–1402.

Chan, D., Fox, N.C., Jenkins, R., Scahill, R.I., Crum, W.R., Rossor, M.N., 2001. Rates of global and regional cerebral atrophy in AD and frontotemporal dementia. Neurology 57, 1756–1763.

Damoiseaux, J., Beckmann, C., Arigita, E., Barkhof, F., Scheltens, P., Stam, C., Smith, S., Rombouts, S., 2008. Reduced resting-state brain activity in the "default network" in normal aging. Cereb. Cortex 18, 1856–1864.

Damoiseaux, J.S., Rombouts, S.A., Barkhof, F., Scheltens, P., Stam, C.J., Smith, S.M., Beckmann, C.F., 2006. Consistent resting-state networks across healthy subjects. Proc. Natl. Acad. Sci. U. S. A. 103, 13848–13853.

Davis, S.W., Dennis, N.A., Daselaar, S.M., Fleck, M.S., Cabeza, R., 2008. Que PASA? The posterior-anterior shift in aging. Cereb. Cortex 18, 1201–1209.

Dennis, N.A., Cabeza, R., 2008. Neuroimaging of healthy cognitive aging, in: Salthouse, T.A., Craik, F.E.M. (Eds.), Handbook of Aging and Cognition, third ed. Psychological Press, New York, pp. 1–56.

Filippini, N., MacIntosh, B.J., Hough, M.G., Goodwin, G.M., Frisoni, G.B., Smith, S.M., Matthews, P.M., Beckmann, C.F., Mackay, C.E., 2009. Distinct patterns of brain activity in young carriers of the APOE-epsilon4 allele. Proc. Natl. Acad. Sci. U. S. A. 106, 7209–7214.

Gili, T., Cercignani, M., Serra, L., Perri, R., Giove, F., Maraviglia, B., Caltagirone, C., Bozzali, M., 2011. Regional brain atrophy and functional disconnection across Alzheimer's disease evolution. J. Neurol. Neurosurg. Psychiatry 82, 58–66.

Glover, G.H., Law, C.S., 2001. Spiral-in/out BOLD fMRI for increased SNR and reduced susceptibility artifacts. Magn. Reson. Med. 46, 515–522.

Good, C.D., Johnsrude, I.S., Ashburner, J., Henson, R.N., Friston, K.J., Frackowiak, R.S., 2001. A voxel-based morphometric study of ageing in 465 normal adult human brains. Neuroimage 14, 21–36.

Greicius, M.D., Srivastava, G., Reiss, A.L., Menon, V., 2004. Default-mode network activity distinguishes Alzheimer's disease from healthy aging: evidence from functional MRI. Proc. Natl. Acad. Sci. U. S. A. 101, 4637–4642.

Jenkinson, M., Bannister, P., Brady, M., Smith, S., 2002. Improved optimization for the robust and accurate linear registration and motion correction of brain images. Neuroimage 17, 825–841.

Leech, R., Kamourieh, S., Beckmann, C.F., Sharp, D.J., 2011. Fractionating the default mode network: distinct contributions of the ventral and dorsal posterior cingulate cortex to cognitive control. J. Neurosci. 31, 3217–3224.

Littow, H., Elseoud, A.A., Haapea, M., Isohanni, M., Moilanen, I., Mankinen, K., Nikkinen, J., Rahko, J., Rantala, H., Remes, J, Starck, T., Tervonen, O., Veijola, J., Beckmann, C., Kiviniemi, V.J., 2010. Age-Related Differences in Functional Nodes of the Brain Cortex—A High Model Order Group ICA Study. Front Syst. Neuroscience, 4. pii: 32.

McKhann, G., Drachman, D., Folstein, M., Katzman, R., Price, D., Stadlan, E.M., 1984. Clinical diagnosis of Alzheimer's disease: report of the NINCDS-ADRDA Work Group under the auspices of Department of Health and Human Services Task Force on Alzheimer's Disease. Neurology 34, 939–944.

Nichols, T.E., Holmes, A.P., 2002. Nonparametric permutation tests for functional neuroimaging: a primer with examples. Hum. Brain Mapp. 15, 1–25.

Oakes, T.R., Fox, A.S., Johnstone, T., Chung, M.K., Kalin, N., Davidson, R.J., 2007. Integrating VBM into the General Linear Model with voxelwise anatomical covariates. Neuroimage 34, 500–508.

Petrella, J.R., Sheldon, F.C., Prince, S.E., Calhoun, V.D., Doraiswamy, P.M., 2011. Default mode network connectivity in stable vs progressive mild cognitive impairment. Neurology 76, 511–517.

Qi, Z., Wu, X., Wang, Z., Zhang, N., Dong, H., Yao, L., Li, K., 2010. Impairment and compensation coexist in amnestic MCI default mode network. Neuroimage 50, 48–55.

Qin, P., Liu, Y., Shi, J., Wang, Y., Duncan, N., Gong, Q., Weng, X., Northoff, G., 2011. Dissociation between anterior and posterior cortical regions during self-specificity and familiarity: A combined fMRI-meta-analytic study. Hum. Brain Mapp., doi:10.1002/hbm.21201.

Raichle, M.E., MacLeod, A.M., Snyder, A.Z., Powers, W.J., Gusnard, D.A., Shulman, G.L., 2001. A default mode of brain function. Proc. Natl. Acad. Sci. U. S. A. 98, 676–682.

Seeley, W.W., Crawford, R.K., Zhou, J., Miller, B.L., Greicius, M.D., 2009. Neurodegenerative diseases target large-scale human brain networks. Neuron 62, 42–52.

Serra, L., Cercignani, M., Petrosini, L., Basile, B., Perri, R., Fadda, L., Spano, B., Marra, C., Giubilei, F., Carlesimo, G.A., Caltagirone, C., Bozzali, M., 2011. Neuroanatomical Correlates of Cognitive Reserve in Alzheimer Disease. Rejuvenation Res. 14, 143–151.

Sheline, Y.I., Morris, J.C., Snyder, A.Z., Price, J.L., Yan, Z., D'Angelo, G., Liu, C., Dixit, S., Benzinger, T., Fagan, A., Goate, A., Mintun, M.A., 2010. APOE4 allele disrupts resting state fMRI connectivity in the absence of amyloid plaques or decreased CSF Aβ42. J. Neurosci. 30, 17035–17040.

Smith, S.M., 2002. Fast robust automated brain extraction. Hum. Brain Mapp. 17, 143–155.

Smith, S.M., Jenkinson, M., Woolrich, M.W., Beckmann, C.F., Behrens, T.E., Johansen-Berg, H., Bannister, P.R., De Luca, M., Drobnjak, I., Flitney, D.E., Niazy, R.K., Saunders, J., Vickers, J., Zhang, Y., De Stefano, N., Brady, J.M., Matthews, P.M., 2004. Advances in functional and structural MR image analysis and implementation as FSL. Neuroimage 23, S208–S219.

Smith, S.M., Nichols, T.E., 2009. Threshold-free cluster-enhancement: addressing the problem of threshold dependence in cluster inference. Neuroimage 44, 83–98.

Solé-Padullés, C., Bartrés-Faz, D., Junqué, C., Vendrell, P., Rami, L., Clemente, I.C., Bosch, B., Villar, A., Bargalló, N., Jurado, M.A., Barrios, M., Molinuevo, J.L., 2009. Brain structure and function related to cognitive reserve variables in normal aging, mild cognitive impairment and Alzheimer's disease. Neurobiol. Aging 30, 1114–1124.

Sorg, C., Riedl, V., Mühlau, M., Calhoun, V.D., Eichele, T., Läer, L., Drzezga, A., Förstl, H., Kurz, A., Zimmer, C., Wohlschläger, A.M., 2007. Selective changes of resting-state networks in individuals at risk for Alzheimer's disease. Proc. Natl. Acad. Sci. U. S. A. 104, 18760–18765.

Sorg, C., Riedl, V., Perneczky, R., Kurz, A., Wohlschläger, A.M., 2009. Impact of Alzheimer's disease on the functional connectivity of spontaneous brain activity. Curr. Alzheimer Res. 6, 541–553.

Strittmatter, W.J., Saunders, A.M., Schmechel, D., Pericak-Vance, M., Enghild, J., Salvesen, G.S., Roses, A.D., 1993. Apolipoprotein E: high-avidity binding to beta-amyloid and increased frequency of type 4 allele in late-onset familial Alzheimer disease. Proc. Natl. Acad. Sci. U. S. A. 90, 1977–1981.

Supekar, K., Menon, V., Rubin, D., Musen, M., Greicius, M.D., 2008. Network analysis of intrinsic functional brain connectivity in Alzheimer's disease. PLoS Comput. Biol. 4, e1000100

Uddin, L.Q., Kelly, A.M., Biswal, B.B., Xavier Castellanos, F., Milham, M.P., 2009. Functional connectivity of default mode network components: correlation, anticorrelation, and causality. Hum. Brain Mapp. 30, 625–637.

Veer, I.M., Beckmann, C.F., van Tol, M.J., Ferrarini, L., Milles, J., Veltman, D.J., Aleman, A., van Buchem, M.A., van der Wee, N.J., Rombouts, S.A., 2010. Whole brain resting-state analysis reveals decreased functional connectivity in major depression. Front. Syst. Neurosci., 4. pii: 41.

Wang, K., Liang, M., Wang, L., Tian, L., Zhang, X., Li, K., Jiang, T., 2007. Altered functional connectivity in early Alzheimer's disease: a resting-state fMRI study. Hum. Brain Mapp. 28, 967–978.

Wang, L., Zang, Y., He, Y., Liang, M., Zhang, X., Tian, L., Wu, T., Jiang, T., Li, K., 2006. Changes in hippocampal connectivity in the early stages of Alzheimer's disease: evidence from resting state fMRI. Neuroimage 31, 496–504.

Westlye, E.T., Lundervold, A., Rootwelt, H., Lundervold, A.J., Westlye, L.T., 2011. Increased Hippocampal Default Mode Synchronization during Rest in Middle-Aged and Elderly APOE {varepsilon}4 Carriers: Relationships with Memory Performance. J. Neurosci. 31, 7775–7783.

Whitfield-Gabrieli, S., Moran, J.M., Nieto-Castañón, A., Triantafyllou, C., Saxe, R., Gabrieli, J.D., 2011. Associations and dissociations between default and self-reference networks in the human brain. Neuroimage 55, 225–232.

Zhang, H.Y., Wang, S.J., Liu, B., Ma, Z.L., Yang, M., Zhang, Z.J., Teng, G.J., 2010. Resting brain connectivity: changes during the progress of Alzheimer disease. Radiology 256, 598–606.

Zhang, H.Y., Wang, S.J., Xing, J., Liu, B., Ma, Z.L., Yang, M., Zhang, Z.J., Teng, G.J., 2009. Detection of PCC functional connectivity characteristics in resting-state fMRI in mild Alzheimer's disease. Behav. Brain Res. 197, 103–108.

Zhang, Y., Brady, M., Smith, S., 2001. Segmentation of brain MR images through a hidden Markov random field model and the expectation-maximization algorithm. IEEE Trans. Med. Imaging 20, 45–57.

Zhou, J., Greicius, M.D., Gennatas, E.D., Growdon, M.E., Jang, J.Y., Rabinovici, G.D., Kramer, J.H., Weiner, M., Miller, B.L., Seeley, W.W., 2010. Divergent network connectivity changes in behavioural variant frontotemporal dementia and Alzheimer's disease. Brain 133, 1352–1367.